Crystallization of Sunflower Oil Waxes

S. Martini* and M.C. Añón

Centro de Investigación y Desarrollo en Criotecnología de Alimentos (CIDCA) (UNLP-CONICET), La Plata, 1900, Argentina

ABSTRACT: Activation free energies of nucleation (ΔG_c) were calculated using induction times of crystallization measurements. Results showed that ΔG_c decreased exponentially as wax concentration increased at a constant crystallization temperature (T_c). In contrast, for a constant supersaturation, ΔG_c increased from 12 to 22°C but decreased between 22 and 35°C. Melting behavior of purified waxes and solutions of purified waxes in sunflower oil were studied by DSC after crystallization at fast and slow cooling rates (20 and 1°C/min, respectively). Low supercooling temperatures (T_c > 65°C) showed an increase in the onset temperature (T_o) as T_c increased for both fast and slow cooling rates. Broader peaks were obtained for samples crystallized at a slow cooling rate at the same T_c. Regarding the solutions of waxes in sunflower oil, the wax concentration (supersaturation of the system) controlled crystallization as well as T_c. As T_c increased, the enthalpy (ΔH) decreased at a constant wax concentration. When wax concentration decreased, ΔH decreased at a constant T_c. For a low driving force, a small shoulder was obtained in the DSC diagrams owing to some type of fractionation. These results showed that wax crystallization is affected by different experimental parameters, such as T_c and cooling rate, depending on the wax concentration of the sample.

Paper no. J10321 in *JAOCS 80*, 525–532 (June 2003).

KEY WORDS: Activation energy of nucleation, cooling rate, differential scanning calorimetry, nucleation, polarized light turbidimetry, sunflower seed oil, waxes.

The quality and stability of vegetable oils such as sunflower oils (SFO) are affected by the presence of minor components. Some of these components are waxes (C_{36}–C_{48}), esters of long-chain saturated FA (C_{20}–C_{22}), and alcohols of C_{24}–C_{28}. Waxes have low solubility in oil at low temperatures and cause turbidity when they crystallize. Therefore, waxes in the oil are eliminated by winterization during the refining process. The introduction of new varieties of sunflower seeds with high oil yields has led to an increase in the efficiency of the wax separation process to avoid turbidity in the refined oil (1). The winterization process is based on the crystallization of waxes present in the oil at a crystallization temperature (isothermal crystallization). Overall, the crystallization process can be divided into two steps: nucleation and growth. Nucleation may be compared with birth: Before any nucleus formation can occur, something must happen in the mother phase—the achievement of supersaturation or supercooling (for nucleation from solutions or from the melt, respectively). Once the nuclei are formed, they grow and develop into crystals. Since there is continuous variation in supersaturation, the system is in continuous evolution: New nuclei may be formed by primary or secondary nucleation, stable crystals can modify their habit, and metastable ones can undergo phase transitions (2). Different processing factors, such as cooling rate and crystallization temperature (T_c) as well as the supersaturation of the system, may influence the crystallization behavior of any system. Studying the influence of these parameters on wax crystallization is quite interesting since the winterization process during SFO refining is very important. Therefore, the aim of the present work was to study both the crystallization and thermal behavior of waxes present in SFO. A polarized laser turbidimeter was used to monitor the crystallization of waxes in order to calculate their activation free energy of nucleation (ΔG_c), and a differential scanning calorimeter was used to study their thermal behavior under different crystallization conditions.

*To whom correspondence should be addressed at CIDCA, Calle 47 y 116, 1900, La Plata, Argentina. E-mail: smartini@dalton.quimica.unlp.edu.ar

MATERIALS AND METHODS

Oil and wax samples. Wax-free SFO was obtained from commercial oil (Molinos Río de la Plata S.A., Buenos Aires, Argentina) by centrifugation (3000 × *g*, 60 min at 0°C). The wax obtained by this procedure was eliminated. The purified wax samples used in this investigation were obtained by filtration (with a Büchner funnel) of samples of crude oil from tank settlings provided by Molinos Río de La Plata, S.A. Waxes were washed three times with petroleum ether at 0°C. Further purification involved hot extractions with hexane followed by centrifugation (3000 × *g*/30 min at 0°C).

Wax solutions. Wax solutions were prepared by dissolving purified wax in wax-free oil. The solutions were heated (90 min at 120°C) and stored at 0°C. Solutions at wax concentrations (C) between 8 and 1000 ppm were used to calculate the induction times of crystallization and thereby the ΔG_c. Wax solutions at 500, 1000, 2500, and 5000 ppm were used to perform the thermal analysis.

Isothermal crystallization. The induction time of crystallization of the wax solutions was measured using an optical setup similar to the one described by Herrera (3). The equipment used a helium–neon laser as the light source and allowed the detection of optically anisotropic crystals (e.g., wax crystals) developed in the sample. The sample was contained in a water-jacketed glass cell equipped with a thermostatic water bath to control temperature. A detailed description of the equipment may be found in References 3–5 and Reference 7. After erasing the crystallization memory of the wax solution (90 min at

120°C), a sample (*ca.* 80 mL) was introduced in the thermostatic cell preset at the T_c (i.e., 12, 22, 30, or 35°C). Crystallization was followed by plotting the laser signal as a function of crystallization time and induction time of crystallization, calculated as described by Martini and Añón (7). Each measurement was done in triplicate, and the mean value was used to calculate ΔG_c.

Calculation of ΔG_c. The activation free energy of nucleation, ΔG_c was evaluated using the following equation (2):

$$J = (\nu\, n_1) \exp(-\Delta G_d/kT) \exp(-\Delta G_c/kT) \quad [1]$$

where J is the rate of nucleation, ν is a frequency term that depends on the rate constant for adding a monomer to an *i*-mer; n_1 is the number of monomers in the system per unit volume, ΔG_d is the activation free energy for volume diffusion, k is the Boltzmann constant per molecule, and T is the temperature in Kelvin. After reaching equilibrium, ΔG_c for a spherical nucleus could be represented by:

$$\Delta G_c = (16/3)\, \pi\, \gamma^3\, \nu^2/(\Delta\mu)^2 \quad [2]$$

where γ is the interfacial free energy of the crystal with respect to the mother phase; ν is the nucleus volume, and $\Delta\mu$ is the chemical potential of the supersaturated solution. Additionally,

$$\Delta\mu = k\, T \ln(C/C_s) \quad [3]$$

where C is the concentration at supersaturation and C_s is the concentration at saturation. The ratio $\beta = C/C_s$ was referred to as the supersaturation parameter. C_s values were 8, 45, 195, and 450 ppm for 12, 22, 30, and 35°C, respectively. C_s was determined—using the optical setup described previously—as the highest concentration that did not crystallize under the experimental conditions assayed.

By combining Equations 1–3, disregarding ΔG_d, and rearranging, the following equation was obtained:

$$J = (\nu\, n_1) \exp - [(16/3)\, \pi\, \gamma^3 \nu^2/ (kT)^3 \ln^2\beta] \quad [4]$$

where J can be considered proportional to the inverse of the induction time of nucleation (τ). Hence, if we plot the $\ln\tau$ corresponding to the different supersaturation values vs. $1/\ln^2\beta$, we should get a straight line. ΔG_c can be calculated from the slope (s) since

$$\Delta G_c = skT/\ln^2\beta \quad [5]$$

Although the slope obtained from this analysis is a constant, ΔG_c is a function of supersaturation and T_c.

Polarized light microscopy. Melted samples of 500, 1000, 2500, and 5000 ppm of waxes in SFO were crystallized at 0, 12, 30, and 35°C at both fast and slow cooling rates (20 and 1°C/min, respectively). After 30 min at T_c, the samples were centrifuged (3000 × *g*, 60 min at T_c) to separate the crystals from the oil and washed twice with cold hexane to eliminate the remaining oil from the crystals. A polarized light microscope with a controlled temperature plate was used to observe the purified crystals. Magnification of 400× was used for all photographs. The X-ray diffraction pattern of these crystals was evaluated.

X-ray diffraction. Samples were analyzed with an X-ray spectrometer (Philips 1730; Philips Argentina S.A., Capital Federal, Argentina) fitted with a system for temperature control (LAUDA UK 30 cryostat; Werklauda, Königshofen, Germany). The temperature of the sample holder placed within the refraction chamber was controlled through a programmable cryostat. Ethylene glycol in water (3:1, vol/vol) was used as coolant. Copper Kα1α2 radiation was used at 40 kV, 20 mA, and scanning velocity of 1°/min from 5 to 50° (6).

DSC. Measurements were carried out in a calorimeter (Pyris™ 1 PerkinElmer calorimeter; PerkinElmer, Chicago, IL). Calibration was carried out with indium and mercury prior to analysis at a heating rate of 10°C/min. The thermograms were analyzed with Pyris™ software for Windows. Samples (purified waxes and different wax solutions in SFO) ranging from 5 to 15 mg were placed in hermetically sealed aluminum pans, heated to 110°C to melt the waxes, and kept there for 10 min. Samples were cooled from this temperature to T_c (0, 12, 22, 30, 35, 65, 70, 71, and 72°C for purified waxes and 0, 12, 22, 30, and 35°C for wax solutions in SFO) at both fast (20°C/min) and slow (1°C/min) cooling rates. After 30 min at T_c, samples were subjected to a heating rate of 10°C/min from T_c to 110°C. A single empty pan was used as a reference. Replicates were performed for each sample to obtain the mean value and to measure the statistical dispersion of each parameter.

RESULTS AND DISCUSSION

Nucleation of waxes. The induction times of nucleation were determined in some wax solutions (7), and these data were used to calculate ΔG_c with Equations 4 and 5. Figure 1 (A–D) shows plots of $\ln\tau$ and $1/\ln^2\beta$ for wax solutions crystallized at 12, 22, 30, and 35°C, respectively. A linear dependence was shown between $\ln\tau$ and $1/\ln^2\beta$ for the samples crystallized at 12°C (Fig. 1A). However, hyperbolic behavior was found at the other T_c (Figs. 1B–D), suggesting the presence of a metastable zone. Thus, there is a critical supersaturation value ($\beta^* = 1.37$, 1.69, 1.55, and 1.33 for crystallization temperatures of 12, 22, 30, and 35°C, respectively) under which the nucleation rate is nearly zero and above which it becomes catastrophic (spontaneous nucleation). For low supersaturation values ($\beta < \beta^*$), a metastable zone exists where the phase transformation kinetics is zero despite the fact that the system is out of equilibrium. In this metastable zone, nucleation is delayed for some time. Metastability depends not only on supersaturation but also on temperature and external factors such as stirring. To calculate ΔG_c, the values of β that represented a metastable zone were neglected and the values of $\beta > \beta^*$ were linearly fitted (R^2 = 0.965, 0.979, 0.991, and 0.965 for 12, 22, 30, and 35°C respectively; $P < 0.01$). From the slope of these lines (s = 0.319, 0.764, 0.385, and 0.129 for 12, 22, 30, and 35°C, respectively),

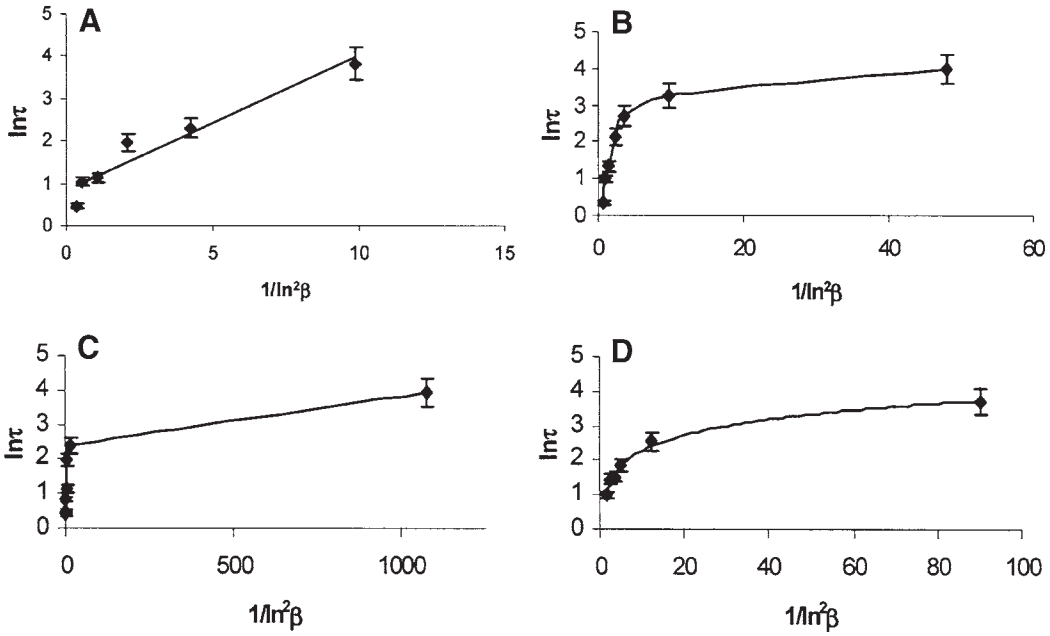

FIG. 1. Plots of lnτ vs. $1/\ln^2\beta$ for wax solutions crystallized at 12, 22, 30, and 35°C (A–D, respectively). τ, induction time of crystallization; β, supersaturation of the system (C/C_s).

ΔG_c could be calculated for each temperature and supersaturation value using Equation 5. Figure 2 shows the variation in ΔG_c with supersaturation for each temperature evaluated. The ΔG_c value decreased exponentially as supersaturation increased for the same T_c. It can be seen that ΔG_c, and therefore the nucleation rate, is strongly dependent on supersaturation at a constant crystallization temperature. To obtain a driving force for crystallization at a constant T_c, the actual concentration in solution must exceed the equilibrium saturation or solubility concentration ($C > C_s$). Thermodynamically, there must be a difference in chemical potential between the concentrated solution and the equilibrium condition. The larger the difference in the chemical potential is, the greater the driving force for crystallization becomes. As crystallization occurs in a closed system, the chemical potential decreases until the equilibrium condition is reached and crystallization ceases (8). When C equals C_s, there is no supersaturation in the system, the nucleation rate is nearly zero, and no induction time is observed since there is no crystallization. However, supersaturation also depends on temperature since solubility (C_s) is a function of this parameter. Thus, it is often difficult to separate the effects of temperature from supersaturation in solution systems. For a given wax concentration, C, the supersaturation (β) decreases as temperature increases since C_s increases. This means that at a constant concentration, the nucleation rate increases while temperature decreases owing to an increase in the driving force, resulting in a higher nucleation rate or, the equivalent, a shorter induction time. Figure 3 shows the variation in ΔG_c with temperature for a constant supersaturation ($\beta = 2$). In this case, the only driving force that affected wax crystallization was the crystallization temperature. $\beta = 2$ was chosen arbitrarily from Figure 2. As can be seen in Figure 3, ΔG_c increased between 12 and 22°C. This means that the induction times were shorter for samples crystallized at 12°C than the ones crystallized at 22°C when the same supersaturated solutions were used. However, ΔG_c decreased when samples were crystallized at temperatures between 22 and 35°C. That is, the nucleation rate increased despite the low value of the driving force. The reason for this occurrence could be that the oil viscosity decreased at high temperatures. Rivarola *et al.* (1) studied oil viscosity behavior and reported an exponential decrease in this parameter between 0 and 35°C. They found that viscosity values were 80, 55, 35, and 30 cP at 12, 22, 30, and 35°C, respectively. Although the viscosity decreased among all the temperatures assayed in this study, when the thermodynamic force was very high (which was the case for high supercooling and low crystallization temperatures), kinetic factors, such as the diffusion of molecules in

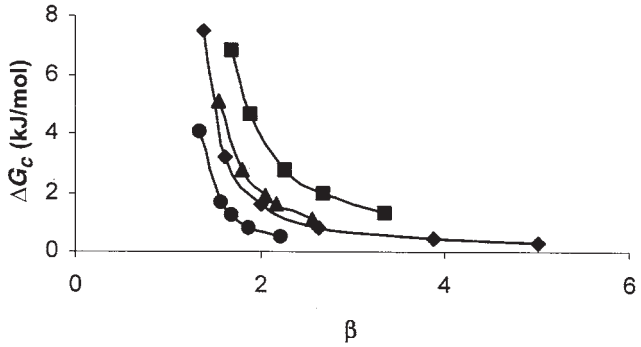

FIG. 2. Activation free energy of nucleation (ΔG_c) vs. supersaturation (β) plot. Samples were crystallized at 12, ◆; 22, ■; 30, ▲; and 35°C, ●, respectively.

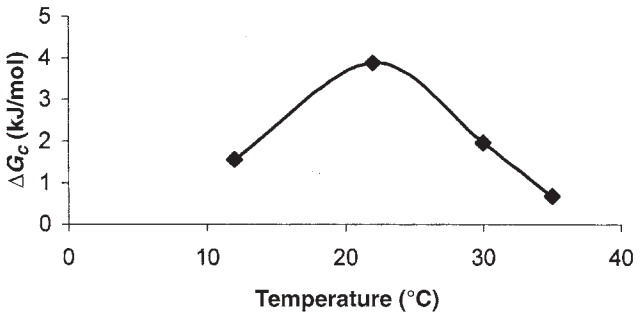

FIG. 3. Variation in ΔG_c with temperature. For abbreviations see Figure 2.

the solution, did not play a key role in the crystallization process. However, when the crystallization temperature increased (e.g., for crystallization temperatures between 30 and 35°C), the driving force was lower and the kinetic factors became the limiting step in the crystallization process. Thus, when performing an experiment at a low driving force and low viscosity, wax molecules can migrate more rapidly in the solutions, resulting in a lower induction time of crystallization since they have less difficulty crossing the interface between the solid and liquid phases to give lower ΔG_c values. Similar results regarding the influence of viscosity on the crystallization kinetics in other systems were reported by Hartel (8).

To avoid studying only the crystallization behavior (nucleation) of the SFO waxes, the thermal behavior of this system was analyzed by DSC as well.

Thermal behavior. (i) Purified waxes. Figure 4A shows DSC melting diagrams of purified waxes crystallized at 35°C at slow (1°C/min) and fast (20°C/min) cooling rates. The peak widths measured at half their height, $\Delta T_{1/2}$, were 3.0 and 2.8°C for the slowly and rapidly cooled samples, respectively, indicating a

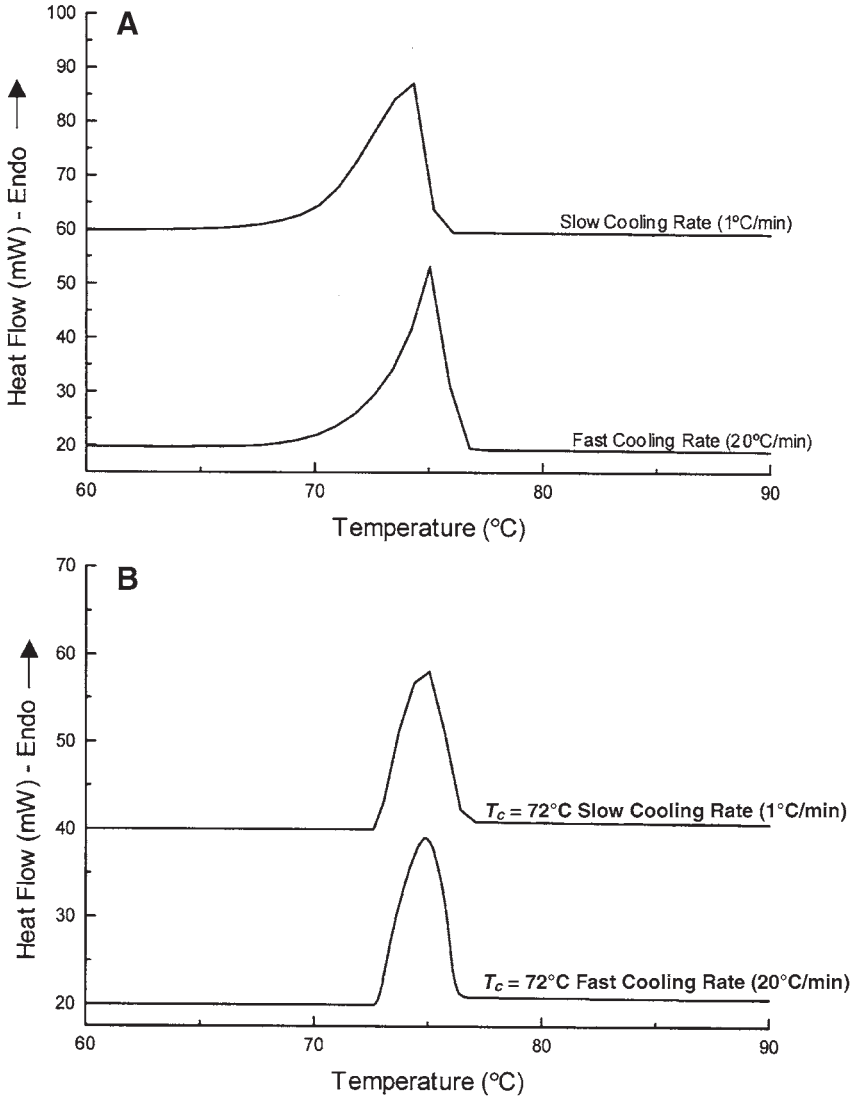

FIG. 4. DSC melting diagrams of purified waxes crystallized at 35°C (A) and 72°C (B) at slow and fast cooling rates (1 and 20°C/min, respectively).

TABLE 1
DSC Melting Curve Parameters of Purified Waxes When Crystallized at Fast (20°C/min) and Slow (1°C/min) Cooling Rates[a]

	Fast cooling rate (20°C/min)			Slow cooling rate (1°C/min)		
T_c (°C)	T_{onset} (°C)	ΔH (J/g)	T_{peak} (°C)	T_{onset} (°C)	ΔH (J/g)	T_{peak} (°C)
35	70.4 ± 0.1	198.54 ± 1.67	74.4 ± 0.5	70.1 ± 0.5	199.82 ± 0.83	74.3 ± 0.5
70	70.7 ± 0.2	175.95 ± 1.41	74.9 ± 0.4	70.7 ± 0.4	174.16 ± 0.71	74.7 ± 0.3
71	71.8 ± 0.5	141.15 ± 1.13	75.0 ± 0.2	71.9 ± 0.5	140.89 ± 0.58	74.9 ± 0.1
72	72.8 ± 0.5	87.39 ± 0.70	74.9 ± 0.4	72.8 ± 0.3	87.11 ± 0.36	74.8 ± 0.5

[a]T_c, crystallization temperature; T_{onset}, onset temperature; T_{peak}, peak temperature; ΔH, enthalpy.

broader peak in the slowly cooled sample. Table 1 shows the parameters (onset and peak temperatures, T_{onset} and T_{peak}, and enthalpies, ΔH) obtained from the DSC diagrams of purified waxes crystallized at different T_c (T_c = 35, 70, 71, and 72°C) at different cooling rates. Purified waxes were also crystallized at 0, 12, 22, 30, and 65°C, and no differences in their melting behavior were observed ($P < 0.05$) when compared with the samples crystallized at 35°C. Figure 4B shows DSC melting thermograms for purified waxes crystallized at T_c = 72°C at fast and slow cooling rates. Although there was no significant difference in T_{onset} values between cooling rates at constant T_c ($P < 0.05$), it can be seen from Figure 4B that the slowly cooled sample gave a small shoulder at low temperatures (left side of the peak of the melting thermogram). $\Delta T_{1/2}$ values were 3.1, 3.0, and 2.3°C for the samples crystallized at a slow cooling rate to 70, 71, and 72°C and 2.8, 3.0, and 2.2°C for the same samples crystallized at a fast cooling rate. These values showed a broader peak in the slowly crystallized samples. When samples were crystallized at 70, 71, and 72°C, T_{onset} increased with T_c (Table 1), and a narrower peak was obtained for a high T_c (Fig. 5A). Samples crystallized at low T_c (35°C) showed more tailing than the ones crystallized at higher temperatures (e.g., 72°C), indicating the presence of low-melting compounds in the samples crystallized at low temperatures. This behavior was found for both cooling rates assayed (Table 1). There was no difference in T_{peak} values ($P < 0.05$) for all samples. Table 1 also shows a decrease in ΔH with an increase in T_c. This result was expected since the driving force decreased with temperature. There was no difference in ΔH values ($P < 0.05$) between different cooling rates at a constant T_c. When purified waxes were crystallized at T_c = 0–65°C, the crystallization process took place at very high supercooling temperatures (T_c too low) and no difference in their thermal behavior was observed. When samples were cooled rapidly to the T_c, crystals did not have enough time to rearrange and solid solutions were obtained, showing a narrow peak. When samples were crystallized at slow cooling rates, the system was under equilibrium conditions that facilitated the molecular organization of waxes with similar chemical compositions and a small shoulder or a broader peak was obtained at lower temperatures. This behavior was found in other lipid systems (9).

(ii) Wax solutions. Table 2 shows DSC melting curve parameters for solutions of 5000, 2500, 1000, and 500 ppm of waxes in SFO crystallized at different T_c at a fast cooling rate. In wax solutions the driving force is not only the T_c (supercooling) but also the wax concentration (supersaturation of the system). Enthalpy values (reported in J/g of solution) decreased with low concentrations at the same T_c owing to a lower driving force (β). Figure 5B shows the melting curves of a solution of 5000 ppm of waxes in SFO when crystallized at different T_c (0, 12,

TABLE 2
DSC Melting Curve Parameters of Wax Solutions in Sunflower Oil When Crystallized at a Fast Cooling Rate (20°C/min) at Different T_c

	5000 ppm			2500 ppm		
T_c (°C)	T_{onset} (°C)	ΔH (J/g)	T_{peak} (°C)	T_{onset} (°C)	ΔH (J/g)	T_{peak} (°C)
0	40.9	0.91	49.2	41.4	0.51	46.4
12	40.1	0.91	48.9	31.9	0.44	46.2
22	39.3	0.83	48.7	35.1	0.29	44.5
30	41.9	0.35	48.7	41.0	0.17	45.3
35	45.9	0.13	49.3	43.2	0.05	46.2
	1000 ppm			500 ppm		
0	46.7	0.39	50.2	43.8	0.21	50.5
12	45.5	0.32	50.2	44.0	0.20	50.6
22	47.2	0.12	52.5	45.0	0.04	52.0
30	—	—	—	—	—	—
35	—	—	—	—	—	—

[a]Values reported are means of duplicates with a SE of 1% for temperature determinations and 5% in enthalpy calculations. For abbreviations see Table 1.

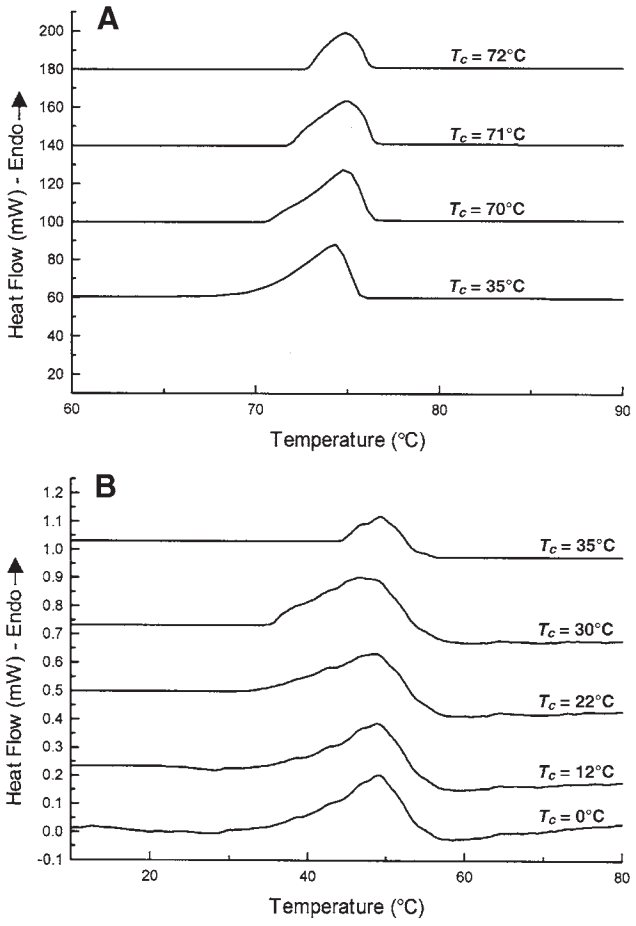

FIG. 5. DSC melting diagrams of (A) purified waxes crystallized at crystallization temperatures (T_c) = 35, 70, 71, and 72°C at a fast cooling rate (20°C/min) and (B) 5000 ppm of waxes in sunflower oil crystallized at 0, 12, 22, 30, and 35°C at a fast cooling rate.

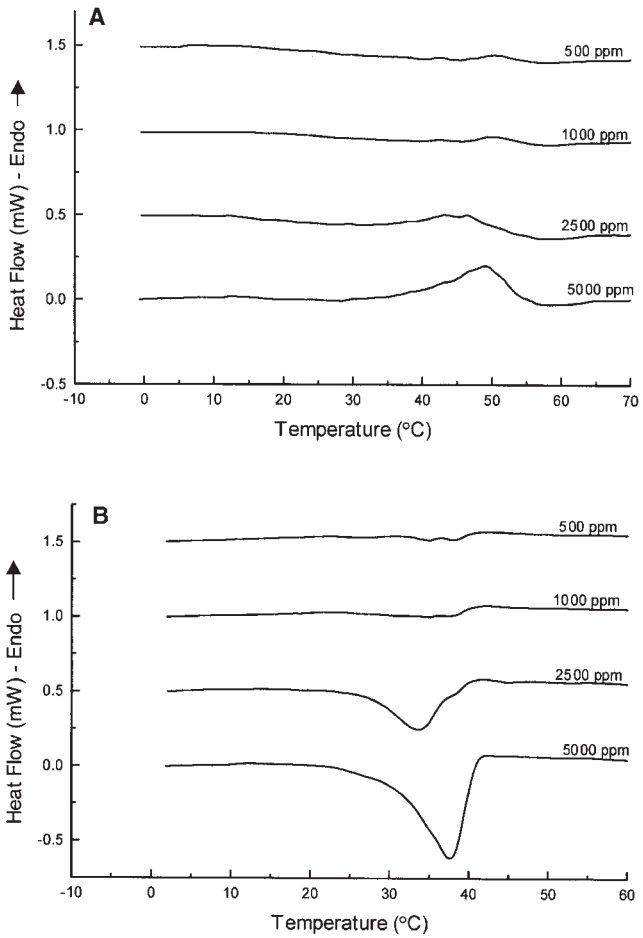

FIG. 6. DSC melting (A) and crystallization (B) behavior of different wax solutions when crystallized at a 0°C at fast cooling rate (20°C/min).

22, 30, and 35°C). In this figure we can observe the effect of the T_c on wax crystallization. When T_c increased, the peak area was smaller; the supersaturation of the system (β) decreased (less driving force) owing to the increase in wax concentration at saturation (C_s) with T_c, which resulted in a low driving force and therefore in lower enthalpies. The same behavior was observed in all the solutions assayed. The increase in T_c resulted in a narrower peak, as observed with the purified waxes.

Figure 6A shows the melting behavior for different wax solutions at T_c = 0°C. We can analyze the effect of concentration on wax crystallization since the only driving force is the supersaturation of the system. Because T_c was constant, C_s is constant too; therefore, the driving force could be determined by the concentration of the solution. When the wax concentration decreased, the peaks become smaller and broader and a shoulder can be seen in the samples with 2500, 1000, and 500 ppm wax. For a constant wax concentration, enthalpies decreased while T_c increased, since both parameters (β and T_c) resulted in a lower driving force, and smaller amounts of waxes were obtained. The crystallization process of these solutions was also assessed by DSC. T_{onset} and T_{peak} were constant among different T_c (T_{onset} = 40.7 ± 0.1, 37.6 ± 0.4, 40.3 ± 0.1, and 40.4 ± 0.1°C for the solutions of 5000, 2500, 1000, and 500 ppm of waxes in SFO, respectively; T_{peak} = 38.0 ± 0.3, 34.3 ± 0.4, 36.4 ± 1.8, and 38.1 ± 0.1°C for the same solutions). Crystallization enthalpy values decreased with a high T_c and low concentration as shown by the melting behavior data (Table 2). Figure 6B shows the crystallization thermograms obtained for different wax solutions crystallized at 0°C. When the wax concentration decreased, a shoulder appeared at high temperatures, giving rise to two different peaks for the 500 ppm solution. This behavior and the melting profiles of the same solutions can be explained by the fractionation of the waxes present in the solution when the driving force decreased.

In Figure 7 are photographs of purified wax crystals obtained from a 5000 ppm solution crystallized at 0, 12, 22, 30, and 35°C (A–E, respectively). Purified crystals of solutions of 2500, 1000, and 500 ppm wax crystallized at 0°C were also analyzed (F–H, respectively). Different morphologies were observed between the 5000 ppm solution crystallized at 0°C and the same solution crystallized at the other temperatures (12, 22, 30, and 35°C). Larger and denser crystals were found in the

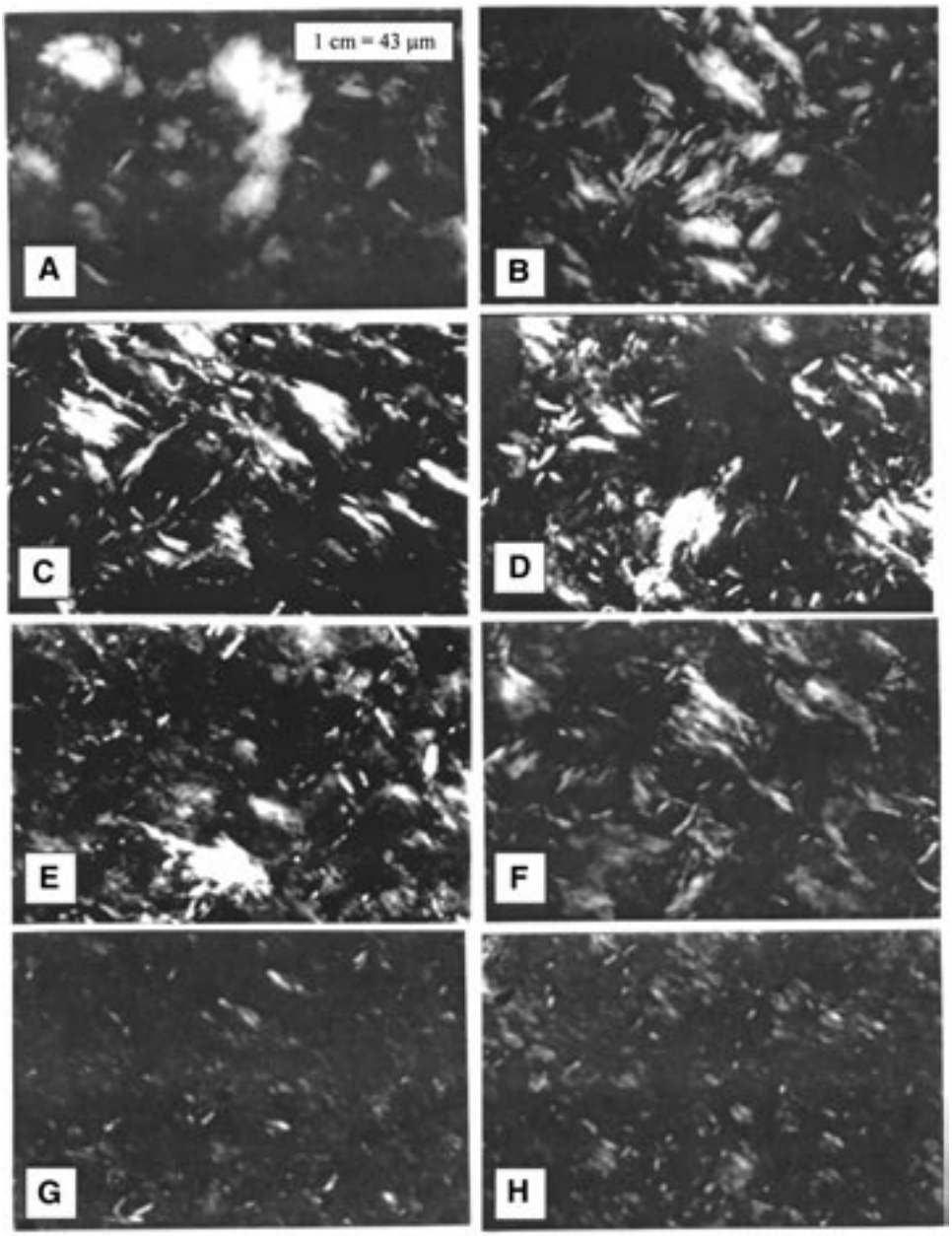

FIG. 7. Purified wax crystals of a 5000 ppm solution crystallized at 0, 12, 22, 30, and 35°C (A–E, respectively), and purified crystals of wax solutions (2500, 1000, and 500 ppm) crystallized at 0°C (F–H, respectively). Magnification: 400×.

sample crystallized at 0°C. When the wax concentration decreased, crystals showed a more defined morphology (Fig. 7G,H). Wax solutions were crystallized at 0°C at the slow cooling rate (1°C/min). DSC melting parameters were: T_{onset} = 39.2 ± 0.4 and 31.7 ± 0.3°C; T_{peak} = 48.6 ± 0.5 and 45.2 ± 0.4°C; and ΔH = 0.80 ± 0.01 and 0.35 ± 0.01 J/g for the 5000 and 2500 ppm solutions, respectively. No peaks were obtained in the 1000 and 500 ppm solutions, and although the peaks obtained in the 5000 and 2500 ppm solutions were very small, a small shoulder was found at higher temperatures in the slowly crystallized samples. In all cases, the shoulders observed were not due to polymorphic transformations since X-ray diffraction analysis of the crystals showed no differences. Two peaks at 4.14 and 3.72 Å were found in all the samples.

Summarizing the study of wax crystallization in SFO, we can state that this process is affected by two variables: T_c and concentration (supersaturation). Both factors represent the driving force that enables the waxes to crystallize. The knowledge of ΔG_c values is a helpful tool to understand the nucleation process. The results show that ΔG_c varies with supersaturation and T_c. The melting behavior of this system was analyzed by DSC, and some fractionation was observed owing to the presence of high- and low-melting waxes. For solutions of waxes in SFO, the wax concentration (supersaturation of the system)

controlled crystallization as well as T_c. As T_c increased, ΔH decreased at a constant wax concentration. When the wax concentration decreased, ΔH decreased at a constant T_c and the melting curves became broader, again indicating the presence of some type of fractionation.

ACKNOWLEDGMENTS

The authors wish to thank the National Research Council from Argentina for the Ph.D. fellowship granted to Silvana Martini. Dr. Añón is Superior Researcher of the National Research Council of Argentina (CONICET). This work was performed under financial support of the project PID-BID 0357 (FONCyT–ANPCyT, Argentina).

REFERENCES

1. Rivarola, G., M.C. Añón and A. Calvelo, Crystallization of Waxes During Sunflowerseed Oil Refining, *J. Am. Oil Chem. Soc. 62*:1508–1513 (1985).
2. Boistelle, R., Fundamentals of Nucleation and Crystal Growth, in *Crystallization and Polymorphism of Fats and Fatty Acids*, edited by N. Garti, and K. Sato, Marcel Dekker, New York, 1988, pp. 189–226.
3. Herrera, M.L., Crystallization Behavior of Hydrogenated Sunflower Seed Oil: Kinetics and Polymorphism, *J. Am. Oil Chem. Soc. 71*:1255–1260 (1994).
4. Chong, C.L., and K. Sato, Kinetic Study of Palm Oil Crystallization, *INFORM 4*:537 (1993) (abstract).
5. Herrera, M.L., and K. Sato, Kinetic Study of Crystallization of Hydrogenated Sunflower-Seed Oil, *Ibid. 5*:553 (1994) (abstract).
6. Liu, H., C.G. Biliaderis, R. Przybylski, and N.A.M. Eskin, Phase Transitions of Canola Oil Sediment, *J. Am. Oil Chem. Soc. 70*:441–448 (1993).
7. Martini, S., and M.C. Añón, Determination of Wax Concentration in Sunflower Seed Oil, *Ibid. 77*:1087–1092 (2000).
8. Hartel, R.W., Nucleation, in *Crystallization in Foods*, Aspen Publishers, Gaithersburg, MD, 2001, pp. 153, 159.
9. Martini, S., M.L. Herrera, and R.W. Hartel, Effect of Cooling Rate on Nucleation Behavior of Milk Fat–Sunflower Oil Blends, *J. Agric. Food Chem. 49*:3223–3229 (2001).

[Received May 3, 2002; accepted February 11, 2003]